Dinuclear Platinum Complexes Form a Novel Intrastrand Adduct with d(GpG), an *anti*−*syn* Conformation of the Macrochelate As Observed by NMR and Molecular Modeling

Yun Qu,[†] Marieke J. Bloemink,[‡] Jan Reedijk,[‡] Trevor W. Hambley,[§] and Nicholas Farrell*,[†]

Contribution from the Department of Chemistry, Virginia Commonwealth University, Richmond, Virginia 23284, Leiden Institute of Chemistry, Leiden University, 2300 RA Leiden, The Netherlands, and Department of Inorganic Chemistry, University of Sydney, NSW 2006, Australia

Received May 30, 1996[⊗]

Abstract: Dinuclear platinum complexes form a unique array of DNA adducts including (Pt,Pt) interstrand and (Pt,Pt) intrastrand cross-links. A (Pt,Pt) intrastrand adduct between two adjacent guanines is the structural analog of the major adduct formed by *cis*-DDP. In this study, we examined the kinetics of formation and structure of the (Pt,Pt) intrastrand adduct by following the interaction of $[\{trans\text{-}PtCl(NH_3)_2\}_2\{\mu\text{-}H_2N(CH_2)_nNH_2\}]^{2+}$ (1,1/t,t, n = 2−6) with d(GpG) using NMR spectroscopy and by molecular modeling. Initial coordination, to either the 5′-G or the 3′-G, is relatively fast compared to the second binding step, ring closure to the macrochelate adduct (*i.e.*, [1,1/t,t]−d(GpG)−N7(1),N7(2)). The rate of ring closure depends on the chain length of the diamine linker. Complexes linked by a longer diamine chain (n = 4−6) react faster and produce a higher yield of macrochelate compared to the shorter n = 2, 3 diamine linkers. The structure of the (Pt,Pt) intrastrand adduct is significantly different from the *cis*-DDP−d(GpG) chelate. The major difference is the presence of a *syn*-orientated G base (observed for 1,1/t,t−(GpG) macrochelates of n = 3 and n = 6). For the macrochelate of [1,1/t,t, n = 3], *i.e.*, $[\{trans\text{-}PtCl(NH_3)_2\}_2\{\mu\text{-}H_2N(CH_2)_3NH_2\}]\{d(GpG)-N7(1),N7(2)\}$, the sugar conformation of the 5′-G(G1) is 28% S, whereas for 3′-G(G2) this value is much higher (69% S). In the corresponding n = 6 macrochelate these values are 55% S and 30% S for G(1) and G(2), respectively. The orientation of the two G bases in the [1,1/t,t]−d(GpG) chelates is best described as tectonic or "stepped head-to-head". The structure helps explain the flexible bending in DNA induced by the dinuclear platinum complexes in contrast to the rigid directed bend into the major groove caused by *cis*-DDP.

Introduction

The utility of cisplatin (*cis*-$[PtCl_2(NH_3)_2]$, *cis*-DDP) in the clinical treatment of cancer is well established.[1,2] Structural analogs of *cis*-DDP do not show a greatly altered spectrum of clinical efficacy in comparison to the parent drug.[3,4] With respect to DNA binding, all *cis*-DDP analogs produce an array of adducts very similar to those of *cis*-DDP and it is therefore not surprising that they induce similar biological consequences.[5] The major adduct of *cis*-DDP is a 1,2-intrastrand cross-link between adjacent guanines.[6−8] This *cis*-DDP−d(GpG) adduct produces a rigid, directed bend 30−35° into the major groove of DNA, which is recognized by damage recognition proteins containing the HMG-binding domain.[9,10] The structural features of the intrastrand adduct have been confirmed by the single-crystal X-ray structure determination of the dodecamer d(CCTCTG*G*TCTCC)−d(GGAGACCAGAGG) platinated at the indicated G*.[11] An NMR structure on d(CCTG*G*TCC)−d(GGACCAGG) also confirmed the DNA bending.[12]

At this stage, it is clear that new clinically useful platinum compounds most likely will not be analogs of the general *cis*-$[PtCl_2(NH_3)_2]$ structure. Our studies on new classes of platinum antitumor agents structurally different from *cis*-DDP have been driven by the hypothesis that alteration of the antitumor activity will be achieved by alteration of the mode of DNA binding in comparison to *cis*-DDP. Dinuclear platinum complexes are of special interest, because they show high activity in vitro and in vivo against tumor cell lines resistant to *cis*-DDP.[13−15] The DNA-binding properties of dinuclear platinum complexes are affected by changing the diamine chain length and the coordination spheres.[16−19] Dinuclear platinum complexes with two

[†] Virginia Commonwealth University.
[‡] Leiden University.
[§] University of Sydney.
[⊗] Abstract published in *Advance ACS Abstracts,* September 1, 1996.

(1) Farrell, N. In *Transition Metal Complexes as Drugs and Chemotherapeutic Agents*; James, B. R., Ugo, R., Eds.; Reidel-Kluwer: Dordrecht, The Netherlands, 1989; pp 46−66.
(2) Reed, E.; Kohn, K. W. In *Cancer Chemotherapy−Principles and Practice*; Chabner, B. A., Collins, J., Eds.; Lippincott, J. B.; Philadelphia, PA, 1990; pp 465−490.
(3) Christian, M. C. *Semin. Oncol.* **1992**, *19*, 720−733.
(4) (a) Dorr, R. T.; Noel, K. *Princ. Pract. Gynecol. Oncol. Updates* **1993**, *1*, 1−14. (b) Reedijk, J. *J. Chem. Soc., Chem. Commun.* **1996**, 801−806.
(5) Ozols, R. F.; Bunn, P. A., Jr.; Comis, R. L. *Semin. Oncol.* **1994**, *21*, 1−92.
(6) Bloemink, M. J.; Reedijk, J. *Metal Ions in Biological System*; Sigel, H., Sigel, A., Eds.; Marcel Dekker, Inc.: New York, 1996; Vol. 32, pp 641−685.
(7) Sundquist, W. I.; Lippard, S. J. *Coord. Chem. Rev.* **1990**, *100*, 293−322.
(8) Comess, K. M.; Lippard, S. J. In *Molecular Aspects of Anticancer Drug−DNA Interactions*; Neidle, S. J., Waring, M., Eds.; CRC Press: Boca Raton, FL, 1993; Vol. 1, p 134.
(9) Pil, P. M.; Lippard, S. J. *Science* **1992**, *256*, 234−237.
(10) Whitehead, J. P.; Lippard, S. J. *Met. Ions Biol. Syst.* **1996**, *32*, 687.
(11) Takahara, P. M.; Rosenzweig, A. C.; Frederick, C. A.; Lippard, S. J. *Nature* **1995**, *377*, 649−652.
(12) Yang, D.; van Boom, S. S. G. E.; Reedijk, J.; van Boom, J. H.; Wang, A. H.-J. *Biochemistry* **1995**, *34*, 12912−12920.
(13) Farrell, N.; Qu, Y.; Hacker, M. P. *J. Med. Chem.* **1990**, *33*, 2179−2184.
(14) Hoeschele, J. D.; Kraker, A. J.; Qu, Y.; van Houten, B.; Farrell, N. In *Molecular Basis of Specificity in Nucleic Acid−Drug Interactions*; Pullman, B., Jortner, J., Eds.; Kluwer Academic Press: Dordrecht, The Netherlands, 1990; pp 301−321.
(15) Farrell, N. *Cancer Invest.* **1993**, *11*, 578−589.

S0002-7863(96)01823-9 CCC: $12.00

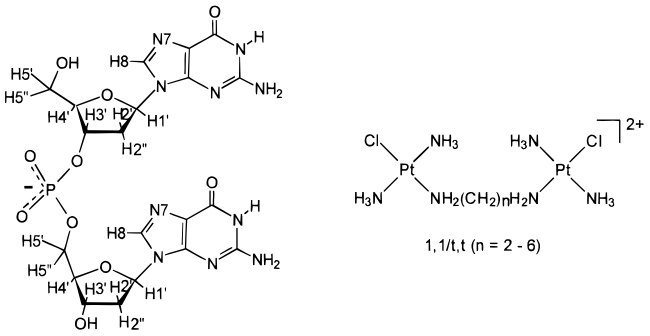

Figure 1. Structures of $[\{trans\text{-}PtCl(NH_3)_2\}_2\{\mu\text{-}NH_2(CH_2)_nNH_2\}]^{2+}$ ($n = 2-6$) and d(GpG). The abbreviation used is 1,1/t,t for this series, which presents one unique chloride *trans* to the diamine bridge.

monofunctional coordination spheres, $[\{trans\text{-}PtCl(NH_3)_2\}_2\{\mu\text{-}H_2N(CH_2)_nNH_2\}]^{2+}$, (Figure 1) form both (Pt,Pt) intrastrand and (Pt,Pt) interstrand cross-links.[20,21] The global structural distortions of DNA induced by the dinuclear platinum complexes are recognized only weakly by HMG-like proteins unlike *cis*-DDP.[18,21] These distortions are therefore clearly structurally distinct from *cis*-DDP and vary within the dinuclear platinum family.

The (Pt,Pt) intrastrand adduct is of especial interest because it is the direct structural analog of the major *cis*-DDP adduct. In contrast to *cis*-DDP, site-specific formation of (Pt,Pt)−1,2-d(GpG) intrastrand adducts formed by $[\{trans\text{-}PtCl(NH_3)_2\}_2\{\mu\text{-}H_2N(CH_2)_nNH_2\}]^{2+}$ does not induce a rigid directed bend into the major groove of DNA but, instead, a flexible bend without any directionality is observed.[22] To examine the features distinguishing the mononuclear and dinuclear intrastrand adducts, we have initiated a study of the dependence of chain length in $[\{trans\text{-}PtCl(NH_3)_2\}_2\{\mu\text{-}H_2N(CH_2)_nNH_2\}]^{2+}$ ($n = 2-6$) upon the structure and kinetics of formation of the adduct with d(GpG) and compared this with the earlier results for *cis*-DDP.[23−26] This paper reports on those results.

Experimental Section

Starting Materials. d(GpG) was synthesized by an improved phosphotriester method[27] and used as its sodium salt. The dinuclear platinum complexes $[\{trans\text{-}[PtCl(NH_3)_2\}_2\{\mu\text{-}H_2N(CH_2)_nNH_2\}]^{2+}$ were prepared by literature procedures and characterized by elemental analysis and ^1H and ^{195}Pt NMR spectroscopy.[28]

Reactions. One equivalent of d(GpG) was allowed to react with an equimolar amount of [1,1/t,t] complex at 10^{-5} M in water at 310 K for 5 days in the dark. After purification by HPLC, the samples were lyophilized twice in 99.996% D_2O and dissolved in 99.999% D_2O (Isotec Inc.) for 2D NMR experiments. The reactions were also followed by NMR (5 mM) at 310 K (see NMR Spectroscopy).

Instrumentation. (a) HPLC. The purification and analysis of the reaction products was performed on an ISCO 2350 liquid chromatograph, with 254-nm detection, on a Waters C18 μ-Bondapak (reversed-phase) column, using an $CH_3CO_2NH_4$ (0.01 M)/CH_3CN gradient.

(b) NMR Spectroscopy. 1D ^1H NMR and ^{31}P NMR spectra were run on a Bruker 250 or on a 300 MHz spectrometer. ^1H NMR spectra were referenced to TMS, and ^{31}P NMR spectra were referenced to trimethyl phosphate (TMP). 2D NMR spectra were recorded on a Bruker WM 600 MHz spectrometer or a Varian UNITY 500 MHz spectrometer. The 2D data were processed using the Felix NMR data processing package (Biosym/MSI) on a Silicon Graphics IRIS workstation.

NMR Experiments. (a) 1D ^1H NMR Spectroscopy. A 5 mM sample of each $[\{trans\text{-}PtCl(NH_3)_2\}_2\{\mu\text{-}H_2N(CH_2)_nNH_2\}]^{2+}$ (1,1/t,t) ($n = 2-6$) was allowed to react with 1 equiv of d(GpG) in 99.996% D_2O (Cambridge Scientific) at 37 °C. The reactions were monitored by ^1H NMR spectroscopy. The pH of solutions was 6.3−6.8 without adjusting.

(b) 2D NMR Spectroscopy. 2D-COSY spectra were recorded using the double-quantum-filtered technique[29] at room temperature. A total of 512 t_1 increments each with 2048 t_2 complex points were collected with a sweep width of 6000 Hz. 2D NOESY spectra were recorded using the States/TPPI technique[30] for phase cycling. Several mixing times were used (200, 300, and 400 ms), and the recycle delay was 1.6 s. A total of 256 t_1 increments each with 1024 t_2 complex points were collected at a sweep width of 8000 Hz. Each FID was the average of 64 transients. 2D-NOESY data were collected at room temperature, except for the [1,1/t,t, $n = 3$]−d(GpG) product, which was recorded at 280 K.

Molecular Modeling. The molecules were first constructed in HyperChem[31] using the AMBER force field. The starting models were built by using the following orientations of the bases with respect to the sugars: *anti/syn*, *syn/anti*, and *anti/anti* (*i.e.*, *anti/syn* represents G(1) is *anti*, G(2) is *syn*). Bond lengths of 2.01 Å for Pt−N7 and 2.03 Å for Pt−amine were used. All N−Pt−N angles were started at 90°, and the dihedral angle between the Pt coordination plane and the guanine ring was also set at 90°. Both sets of angles were allowed to fluctuate during the minimizations as were the Pt−N bond lengths. In order to compare the effect of chain length, these three different starting models were built for the macrochelate adducts of both [1,1/t,t, $n = 3$] and [1,1/t,t, $n = 6$].

One of us (T.W.H.) has modified the AMBER force field parameters and developed a molecular mechanics calculation program called MOMEC.[32] Several platinum complexes and platinum−DNA adducts have been calculated by using this modified AMBER force field with success.[33,34] Other workers have also, more recently, modified the AMBER-type force field to give greater consistency between calculated conformational features and solution and/or crystal structures of *cis*-$[Pt(amine)_2(guanine\ nucleobase)_2]$ species.[35] Thus, molecular modeling was performed by using MOMEC with the modified force field. The strain energy was minimized using a modified version of the Newton−Raphson scheme developed by Boyd.[36] Convergence was defined as the point where shifts for the atomic coordinates were less than or equal to 0.001 Å. The calculations were done on a Silicon Graphics IRIS workstation.

(16) Farrell, N.; Qu, Y.; Feng, L.; van Houten, B. *Biochemistry* **1990**, *29*, 9522−9531.
(17) Roberts, J. D.; van Houten, B.; Qu, Y.; Farrell, N. *Nucleic Acids Res*. **1989**, *17*, 9719−9733.
(18) Farrell, N. *In Advances in DNA Sequence Specific Agents*; Hurley, L. H., Chaires, J. B., Eds.; JAI Press Inc.: Greenwich, CT, 1996; pp 187−216.
(19) Farrell, N. *Comments Inorg. Chem*. **1995**, *16*, 373−389.
(20) Zou, Y.; van Houten, B.; Farrell, N. *Biochemistry* **1994**, *33*, 5404−5410.
(21) Farrell, N.; Appleton, T. G.; Qu, Y.; Roberts, J. D.; Soares Fontes, A. P.; Skov, K. A.; Wu, P.; Zou, Y. *Biochemistry* **1995**, *34*, 15480−15486.
(22) Kašpárková, J.; Mellish, K. J.; Qu, Y.; Brabec, V.; Farrell, N. *Biochemistry*, submitted.
(23) den Hartog, J. H. J.; Altona, C.; Chottard, J. C.; Girault, J. P.; Chottard, G.; Lallemand, J. Y.; Mansuy, D.; de Leeuw, F. A. A. M.; Marcelis, A. T. M.; Reedijk, J. *Nucleic Acids Res*. **1982**, *10*, 4715−4730.
(24) Sherman, S. E.; Gibson, D.; Wang, A. H.-J.; Lippard, S. J. *J. Am. Chem. Soc*. **1988**, *110*, 7368−7381.
(25) Sherman, S. E.; Gibson, D.; Wang, A. H.-J.; Lippard, S. J. *Science* **1985**, *230*, 412−417.
(26) Admiraal, G.; van der Veer, J. L.; de Graaff, R. A. G.; den Hartog, J. H. J.; Reedijk, J. *J. Am. Chem. Soc*. **1987**, *109*, 592−594.
(27) van der Marel, G. A., van Boeckel, C. A. A.; Wille, G.; van Boom, J. H. *Tetrahedron Lett*. **1981**, *3887*−3890.
(28) Qu, Y.; Farrell, N. *Inorg. Chem*. **1992**, *31*, 930−932.
(29) Neuhaus, D.; Wagner, G.; Vasak, M.; Kagi, J. H. R.; Wuthrich, K. *Eur. J. Biochem*. **1985**, *151*, 257−273.
(30) States, D. J.; Haberkorn, R. A.; Ruben, D. J. *J. Magn. Reson*. **1982**, *48*, 286−292.
(31) *HyperChem*, Hypercube Inc., Ontario, Canada.
(32) Hambley, T. W. *MOMEC-91, Programme for Strain Energy Minimisation*; University of Sydney, Sydney, Australia, 1991.
(33) Hambley, T. W. *J. Chem. Soc., Chem. Commun*. **1988**, 221−223.
(34) Hambley, T. W. *Inorg. Chem*. **1991**, *30*, 937−942.
(35) Yao, S., Plastaras, J. P., Marzilli, L. G. *Inorg. Chem*. **1994**, *33*, 6061−6077.
(36) Boyd, R. H. *J. Chem. Phys*. **1968**, *49*, 2574−2583.

Table 1. Chemical Shifts (in ppm) of H8[a] and ^{31}P[b] NMR Data of the d(GpG) Chelates of 1,1/t,t Complexes ($n = 2-6$) (pH 6.3−6.8) and *cis*-DDP, Together with Unplatinated d(GpG)

	Gp− (5′-G)		−pG (3′-G)			
complex	H8	ΔH8[c]	H8	ΔH8[c]	Δ[d]	^{31}P
d(GpG)	7.75	0.00	8.00	0.00	0.00	−4.10
cis-DDP	8.32	+0.57	8.54	+0.54	+0.03	−3.35
1,1/t,t, $n = 2$	8.70	+0.95	8.81	+0.81	+0.14	−3.06
1,1/t,t, $n = 3$	8.08	+0.33	8.45	+0.45	−0.12	−4.61
1,1/t,t, $n = 4$	8.62	+0.87	8.65	+0.65	+0.22	−3.42
1,1/t,t, $n = 5$	8.53	+0.78	8.62	+0.62	+0.16	−3.80
1,1/t,t, $n = 6$	8.53	+0.78	8.56	+0.56	+0.22	−3.97

[a] Referenced to TMS. [b] Referenced to TMP. [c] ΔH8 is δ H8 − δ H8(d(GpG)). [d] $\Delta = \Delta$H8(5′-G) − ΔH8(3′-G).

Table 2. ^{1}H Chemical Shifts[a] of the [1,1/t,t, $n = 2$]GG, [1,1/t,t, $n = 3$]GG, and [1,1/t,t, $n = 6$]GG Adducts (pH 6.4, 298 K), Together with the $^3J_{H1'-H2'}$ and $^3J_{H1'-H2''}$ (in Hz)

			H2′($^3J_{H1'-H2'}$)[b]			H5′	
	H8	H1′	H2″($^3J_{H1'-H2''}$)	H3′	H4′	H5″	$(CH_2)_n$ (linker)
[1,1/t,t, $n = 2$]GG							3.16; 3.78
G(1)	8.70	6.33	3.05 (0.0)	5.25	4.13	3.90	
			2.92 (7.3)			3.78	
G(2)	8.81	6.38	2.64 (6.4)	4.75	4.36	4.20	
			2.53 (6.4)				
[1,1/t,t, $n = 3$]GG							2.13; 2.80; 3.20
G(1)	8.08	6.10	3.01 (3.2)	4.77	4.19	3.48	
			2.63 (7.8)			3.36	
G(2)	8.45	6.32	3.05 (5.6)	4.96	4.27	4.16	
			2.66 (5.6)			3.79	
[1,1/t,t, $n = 6$]GG							2.82; 2.77
							2.10; 2.04
							1.72; 1.61
G(1)	8.53	6.36	2.95 (5.5)	4.89	4.32	4.12	
			2.72 (5.5)				
G(2)	8.56	6.21	2.30 (3.9)	4.87	4.14	3.79	
			2.60 (6.8)			3.73	

[a] Referenced to TMS. [b] H2′/H2″ have been assigned stereospecifically; H5′/H5″ were assigned according to Remin and Shugar.[43]

Results

General Observations. For the 1,1/t,t complexes the major product of the reactions with d(GpG) was identified as an N7,-N7 intramolecular macrochelate, in accordance with our previous results.[37] The pH dependence of the H8 chemical shift provided direct evidence for coordination at N7, since no N7 protonation effect was observed around pH 2−3 for the [1,1/t,t]−d(GpG) products (see Figure S1; Figures S1 and S2 are given in Supporting Information)).[38−40] The H8 protons of all [1,1/t,t]-d(GpG) macrochelates are shifted downfield compared to free d(GpG) (see Table 1). The downfield shifts vary with chain length in the following order: (most downfield) ethylenediamine ($n = 2$) > 1,4-butanediamine ($n = 4$) > 1,5-pentanediamine ($n = 5$) ≈ 1,6-hexanediamine ($n = 6$). The apparent systematic downfield shift with increasing chain length is not seen for the 1,3-propanediamine ($n = 3$) product, which is least shifted in comparison to the other adducts.

In general, the H1′ signals of the adducts show complicated patterns indicative of coupling to both H2′ and H2″ protons. See below for details. These results imply a different sugar conformation in comparison to that of the *cis*-DDP-type chelates, where a 100% N-type 5′ sugar is usually observed, identified by values of $^3J_{H1'-H2'} < 1$ Hz.[23] Interestingly, the [1,1/t,t, $n = 2$]−d(GpG) chelate is similar to the structure of cis-DDP−d(GpG) since a 100% N-type conformation is found for the sugar of G(1) ($^3J_{H1'-H2'} = 0$ Hz; see Table 2).

Except for the $n = 3$ adduct, a downfield shift of the ^{31}P signal from −3.06 to −3.97 ppm is observed for all [1,1/t,t]−d(GpG) macrochelates, compared to free d(GpG) (δ^{31}P = −4.1 ppm; see Table 1). The downfield shifts are similar to those for the *cis*-DDP adduct incorporated into di- and tetranucleotides.[23,42] A downfield shift of the main ^{31}P signal in DNA usually indicates an increase in the unwinding angle characterized by changes in R−O−P−OR torsion angles.[43] An unusual upfield shift was observed for the $n = 3$ chelate at −4.61 ppm (Table 1). Upfield ^{31}P signals have also been observed for the adducts of *trans*-[Pt(NH$_3$)$_2$Cl$_2$] with d(GTG) and a hairpin-like structure of *cis*-DDP with d(TCTCGGTCTC).[44,45] Rotation around the exocyclic C5′−C4′ bond plays a key role in positioning the 5′-phosphate group relative to the sugar and base in DNA, thereby dictating to some extent its chemical shift. Upfield chemical shifts such as those noted above have been variously explained by hydration of the phosphate, torsional strain around the torsion angle γ, or the presence of hydrogen bonds.[43,46,47]

Upon coordination to the chiral d(GpG) molecule, the CH$_2$ signals of the diamine linker become inequivalent. For both *n*

(37) Bloemink, M. J.; Reedijk, J.; Farrell, N.; Qu, Y.; Stetsenko, A. I. *J. Chem. Soc., Chem. Commun.* **1992**, 1002−1003.
(38) Chottard, J. C.; Girault, J. P.; Chottard, G.; Lallemand, J. Y.; Mansuy, D. *J. Am. Chem. Soc.* **1980**, *102*, 5565−5572.
(39) Scheller, K. H.; Scheller-Krattiger, V.; Martin, R. B. *J. Am. Chem. Soc.* **1981**, *103*, 6833−6839.
(40) Qu, Y.; Farrell, N. *J. Am. Chem. Soc.* **1991**, *113*, 4851−4857.
(41) Remin, M.; Shugar, D. *Biochem. Biophys. Res. Commun.* **1972**, *48*, 636−642.
(42) Fouts, C. S.; Marzilli, L. G.; Byrd, R. A.; Summers, M. F.; Zon, G.; Shinozuka, K. *Inorg. Chem.* **1988**, *27*, 366−376.
(43) Gorenstein, D. G. In *Phosphorus-31 NMR: Principles and Applications*; Gorenstein, D. G., Ed.; Academic Press: New York, 1984; Chapters 1 and 8.
(44) Boogaard, N.; Altona, C.; Reedijk, J. *J. Inorg. Biochem.* **1993**, *49*, 129−147.
(45) Kline, T. P.; Marzilli, L. G.; Live, D.; Zon, G. *J. Am. Chem. Soc.* **1989**, *111*, 7057−7068.
(46) Lerner, D. B.; Becktel, W. J.; Everett, R.; Goodman, M.; Kearns, D. R. *Biopolymers* **1984**, *23*, 2157−2172.
(47) Altona, C. *Recl. Trav. Chim. Pays-Bas* **1982**, *101*, 413−433.

Scheme 1. Pathways of Formation of the (Pt,Pt)−d(GpG) Intrastrand Adduct of Dinuclear Platinum Complexes[a]

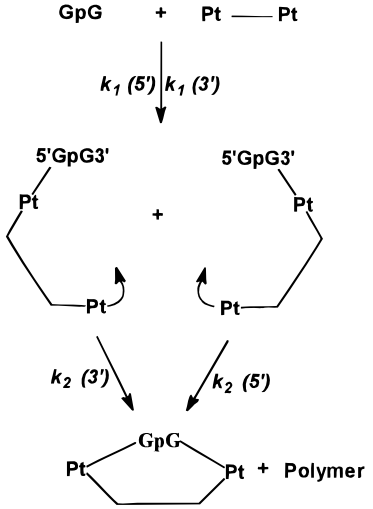

[a] The scheme is in perfect agreement with the NMR studies. Polymer formation occurs through reaction of intermediates with free (unplatinated) dinucleotide.

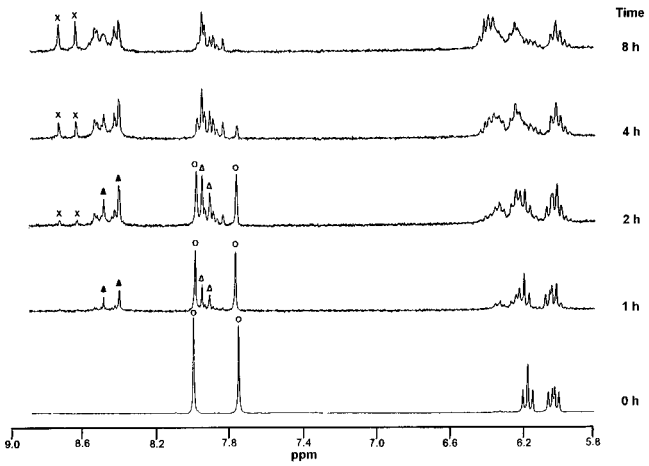

Figure 2. Reaction of (1,1/t,t, $n = 2$) and d(GpG) showing H8 and sugar H1′ protons at 37 °C in D_2O at 5 mM (in reference to TMS): (○) free d(GpG); (△, ▲) intermediates (▲ is platinated G); (×) [Pt,-Pt]−d(GpG) macrochelate. Within 1 h, four peaks appear at 7.88, 7.98, 8.45, and 8.55 ppm, corresponding to the two intermediates *G*pG and Gp*G* (*G* represents platinated guanine). *GpG* (macrochelate) can be detected after ∼2 h.

$= 3$ and $n = 6$ derivatives, separate signals were observed for each unique CH_2 group; (see Table 2).

Kinetic Aspects. The stepwise reaction of the dinuclear platinum complexes of the 1,1/t,t series with d(GpG) may be represented as in Scheme 1. The initial approach of a dinuclear platinum complex to d(GpG) must obviously be monofunctional binding, *i.e.*, platination at either the 5′-G or the 3′-G followed by closure to the macrochelate or competing polymer formation through chain extension.

The time course of the reactions of [{*trans*-$PtCl(NH_3)_2$}$_2${μ-$H_2N(CH_2)_nNH_2$}]$^{2+}$ ($n = 2$ and 6) with d(GpG) followed by ^{1}H NMR spectroscopy are shown in Figures 2 and 3. The spectra are similar in all cases. The H8 peaks of free d(GpG) appear at 7.75 and 8.0 ppm (○). Two new signals appear at 7.88−7.98 ppm (△) and another two appear at 8.45−8.55 ppm (▲). These intermediate signals are assigned to the monofunctionally platinated GpG moieties giving rise to four signals. This pattern is expected from Scheme 1, where the two distinct platinated guanines will be shifted more than the unplatinated

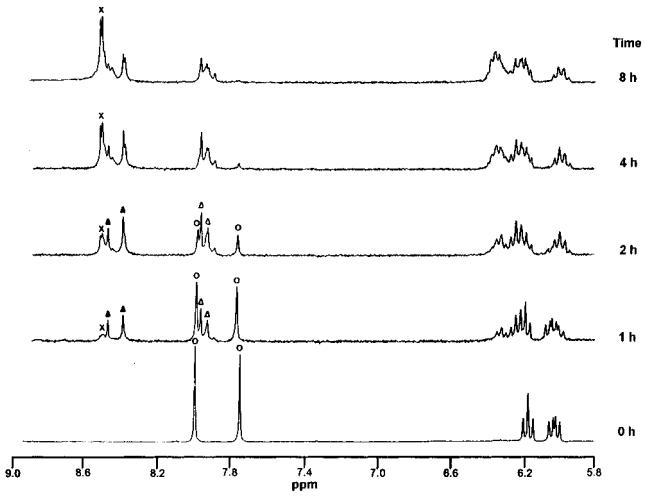

Figure 3. Reaction of (1,1/t,t, $n = 6$) and d(GpG) (5 mM at 37 °C) showing H8 and sugar H1′ protons (in D_2O and referenced to TMS): (○) free d(GpG); (△, ▲) intermediates (▲ is platinated G); (×) *GpG* (macrochelate). The reaction intermediates are *G*pG and Gp*G* (*G* represents N7 platinated guanine); *GpG* can be detected after ∼1 h.

pair.[48] After 1 h, the spectra become more complicated. The intermediates gradually disappear while two new distinctive H8 signals appear (×), corresponding to the intramolecular macrochelate adduct. Other H8 signals apparent in Figures 2 and 3 are assigned to the competing polymer formation and were not investigated further. The disappearance of free d(GpG), and therefore the rate of monoplatination, is essentially independent of chain length and no free dinucleotide is apparent after ∼8 h. However, the intermediate signals can still be seen and thus macrochelate continues to be formed even after the free dinucleotide is all reacted. After 48 h there is no further change in any of the spectra. The rate of appearance of the macrochelate is dependent on chain length. For $n = 2$, the chelate signals begin to appear after ∼2 h, whereas with $n = 6$, the H8 signals of the chelate are apparent already after 1 h. The qualitative rate of formation of the intramolecular macrochelate could be determined from the 1D spectra by measuring the signal intensity of the macrochelate (as judged by intensity of signal relative to the other H8 signals). The order is as follows: $n = 6 > n = 5 > n = 4 > n = 3 > n = 2$. The yield of macrochelate is higher for the longer $n = 6$ diamine chain while the shorter linkers give relatively more polymer as side product (See Figure S2). The overall kinetic profile follows Scheme 1 although no quantitative measurement was attempted because of the difficulty of separating the competing k_1 and k_2 steps (See Scheme 1) as well as the use of D_2O as solvent. The first binding step (k_1) is relatively fast compared to the second reaction step (k_2) and is not affected by the chain length of the diamine linker. The rate of the chelate closure depends on the diamine chain length, being more difficult for the sterically more restricted short chains ($n = 2$, 3).

Structural Analysis. 2D-NOESY and DQF-COSY ^{1}H NMR spectra in D_2O were used to assign the nonexchangeable protons of the $n = 2$, 3, and 6 products (Table 2). The diamine linker spin system and the sugar spin systems could be extracted from the DQF-COSY spectra. The specific assignment of the sugar residues to their respective base was straightforward, *i.e.*, a lack of H5′/H5″−^{31}P coupling for the 5′ sugar and absence of H3′−^{31}P coupling for the 3′ sugar. From the NOESY data, the 5′-G(1) and 3′-G(2) H8 signals could be distinguished and their

(48) Lempers, E. L. M.; Bloemink, M. J.; Brouwer, J.; Kidani, Y.; Reedijk, J. *J. Inorg. Biochem.* **1990**, *40*, 23−35.

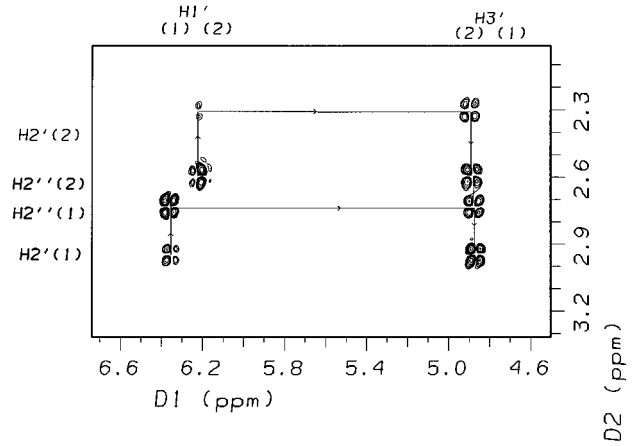

Figure 4. H1′ and H2′/H2″ area of the DQF-COSY spectrum of [1,1/t,t, $n = 6$]GG. The reduced $^3J_{H1'-H2'}$ of G(2) indicates a C3′-endo conformation of the sugar moiety.

relative conformation (*syn/anti*) assigned. The $n = 3$ and $n = 6$ spectral sets were examined in more detail.

[1,1/t,t, *n* = 6]−d(GpG). The COSY spectrum afforded values of $^3J_{H1'-H2'} = {}^3J_{H1'-H2''} = 5.5$ Hz for the 5′-G(1) deoxyribose. For the 3′G(2) deoxyribose, the H1′−H2′ coupling for 3′-G is reduced (3.9 Hz) (see Table 2 and Figure 4). The sugar ring in DNA molecules is in rapid equilibrium on the NMR time scale between S-type (C2′-endo, C3′-exo) and N-type (C2′-exo, C3′-endo) conformers.[49,50] This equilibrium is characterized by the population of S conformers (% S). In B-DNA fragments 80−100% S is found, except for the sugar of the 3′-end residue, which has more conformational freedom and occurs in an approximate 60−70% S/40−30% N equilibrium.[47] An estimate of the percent of S and N conformers was made, using expression 1 for the determination of the fraction of S

$$f_S = (31.5 - \sum 2'')/10.9 \qquad (1)$$

conformers (f_S).[49] Calculation of the sugar conformation using (1) shows that the deoxyribose ring of G(1) is in a N/S equilibrium (*i.e.*, 55% S) and the sugar of G(2) is in a $C_{3'}$-endo orientation (*i.e.*, 30% S).

For G(1) a strong NOE between H8(1) and H2′(1) is present, characteristic of an *anti* orientation around the glycosidic bond (see Figure 5). The absence of the equivalent intraresidual NOE between H8(2) and H2′(2) indicates a change toward the *syn* conformation for the 3′ sugar residue, confirmed by the presence of a strong intraresidual NOE between H8(2) and H1′(2).[51,52]

[1,1/t,t, *n* = 3]−d(GpG). A strong NOE cross-peak between H8(2) and H1′(2) is found, suggesting a *syn* orientation of G(2) (see Figure 6).[52] Since NOE cross-peaks between H8(2) and H2′(2) and H3′(2) are also present, the orientation can partly be *anti*. For G(1), a strong intraresidual NOE cross-peak between H8 and H3′ suggests an *anti* orientation for this base and also a N-type conformation (C_3′-endo) of the sugar.[49] However, the characteristic NOE between the G(1) H8 and its H2′ proton is absent. A possible explanation is that the sugar conformation is "high anti", a variation of the anti conformation resulting from a near eclipse of the $C_{1'}-C_{2'}$ sugar bond with the C_9-C_8 bond of the purine.[50] In this case, a larger H8−H_2′ distance is expected, diminishing any NOE intensity. A high

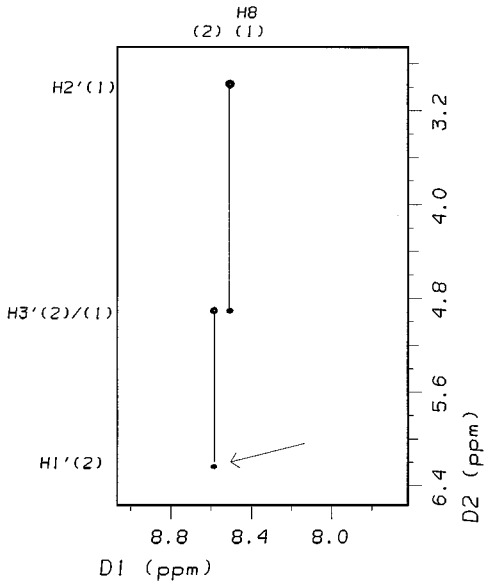

Figure 5. Expanded NOESY spectrum of the [1,1/t,t, $n = 6$]GG adduct. Note the presence of a NOE between H8(2) and H1′(2) and the absence of NOEs from H8(2) toward H2′/H2″, indicative of a *syn*-oriented guanine.

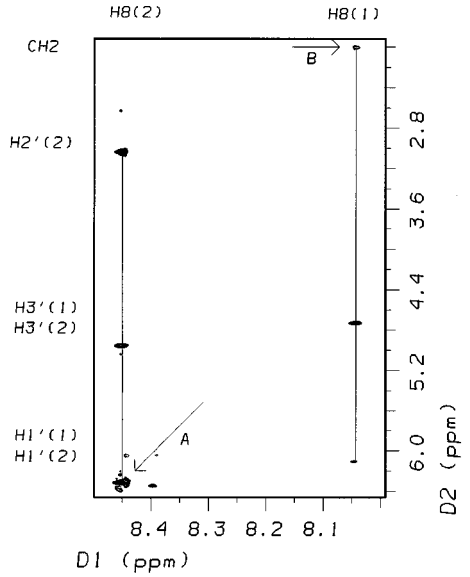

Figure 6. Expanded NOESY spectrum of the [1,1/t,t, $n = 3$]GG adduct. The relative strong NOE between H8(2) and H1′(2) suggests a *syn* orientation of G(2) (arrow A). Also a NOE between the propanediamine linker and H8(1) is indicated (arrow B).

anti conformation has been found for the guanine sugar in the adduct of d(AGA) with the monofunctional [Pt(dien)].[53] As stated above, the inequivalence of the two H_2NCH_2 groups suggests a close orientation of the linker toward d(GpG), confirmed by the presence of a NOE between the central linker protons ($NH_2CH_2CH^*{}_2CH_2NH_2$) and the 5′G(1) H8 of the d(GpG) moiety (see Figure 6).

Molecular Modeling. Model Comparisons. To explain the NMR results and assist in building a three-dimensional structure, various models of the (Pt,Pt)−d(GpG) adducts were built using the approach of Hambley.[32] As a starting point, three models were built with sugar conformations designated as *anti/syn* (i.e., 5′-G(1) is *anti*, 3′-G(2) is *syn*), *syn/anti*, and *anti/anti* since these are the most likely combination of sugar conformations. The

(49) Rinkel, L. J.; Altona, C. *J. Biomol. Struct. Dyn.* **1987**, *4*, 621−649.
(50) Saenger, W. *Principles of Nucleic Acid Structure*; Springer-Verlag: New York, 1984; Chapters 11, 12, and 16.
(51) Orbons, L. P. M.; van der Marel, G. A.; van Boom, J. H.; Altona, C. *Eur. J. Biochem.* **1986**, *161*, 131−139.
(52) Patel, D. J.; Kozlowski, S. A.; Nordheim, A.; Rich, A. *Proc. Natl. Acad. Sci. U.S.A.* **1982**, *79*, 1413−1417.
(53) Admiraal, G.; Alink, M.; Altona, C.; Dijt, F. J.; van Garderen, C. J.; de Graaff, R. A. G.; Reedijk, J. *J. Am. Chem. Soc.* **1992**, *114*, 930−938.

Table 3. Comparison of Energies for the Conformational Adducts of [1,1/t,t, $n = 6$]GG

energy component	energy (kJ/mol)		
	anti/syn	*syn/anti*	*anti/anti*
bond deformation	7.4	7.9	8.4
nonbond interaction	−7.1	0.0	−6.8
valence angle deformation	34.6	36.6	39.3
torsion angle deformation	44.7	36.4	36.3
electrostatic interaction	−262.8	−249.7	−253.1
out-of-plane deformation	0.1	0.0	0.1
hydrogen bond interaction	−15.2	−10.7	−15.3
total strain energy	−198.4	−179.4	−191.1

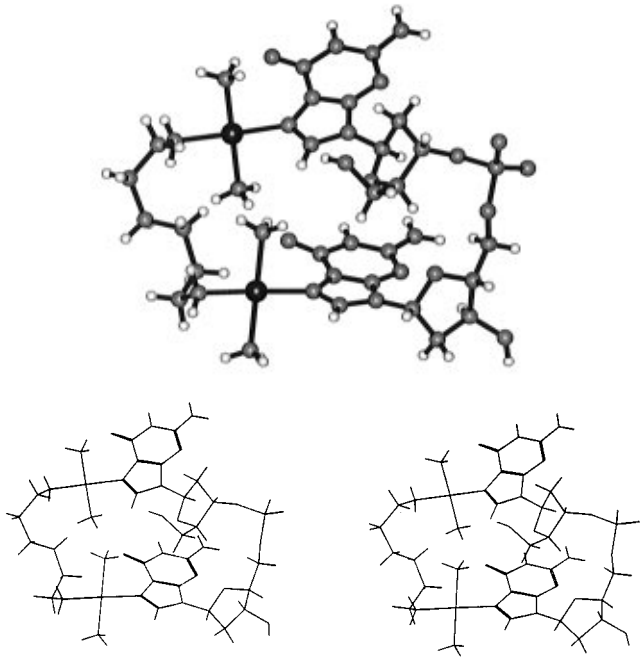

Figure 7. Ball and stick (top) and stereoview (below) of the anti/syn model of [1,1/t,t $n = 6$]-d(GpG). Note the stepped head-to-head orientation of the guanines.

macrochelate complexes are highly flexible and can adopt a large number of conformations. A number of different conformations were considered and many others are undoubtably possible. For the refined models, the strain energy of the *anti/syn* oriented model is lower than the *syn/anti* and *anti/anti* models but the energy differences are such that in solution all would be adopted to some degree. For the $n = 6$ models, the two most energetically favorable models were the *anti/syn* (most stable) and *anti/anti* with an energy difference of $\Delta E = 7$ kJ/mol (See Table 3). Hydrogen bonds between the O6−gaunine and H−NH_3 were found in all models and contribute to the low energy level. Because the NMR results indicated the likelihood of a *anti/syn* arrangement of the sugars, we discuss the structural parameters for this model.

The Anti/Syn Model for the 1,1/t,t $n = 6$-d(GpG) Adduct. Figure 7 shows the stereoviews of the energetically favored *anti/syn* macrochelate, and Table 4 gives the structural parameters derived. In the structure, the orientation of the two guanines is best described as "tectonic" or "stepped head-to-head". The two guanines are still oriented in a head-to-head fashion but are shifted compared to a regular head-to-head structure (see Scheme 2). The H8−H1′ distances are close to 3.5 Å for the G(1) and 2.5 Å for G(2) (Table 4). This result is consistent with the observations of NOEs between H8 and H1′ for the 3′-G(2) but not the 5′-G(1).

Table 4 shows that a small dihedral angle of 25° between the two guanine planes is found in this *anti/syn* model. The dihedral angle between the two Pt−N coordination planes (PtN_4) is 20°, and the dihedral angle between the Pt−N coordination plane and guanine plane is ∼60°. The distance between the two platinum atoms is 6.7 Å (see Table 4) and the N7−N7 distance is 6.6 Å.

Table 4. Distance Values and Angles of the [1,1/t,t, $n = 6$]GG of *anti/syn* Model

Nonbonded Distances (Å)			
$Pt_1\cdots Pt_2$	6.7	H8···H1′(5′-G)	3.5
O6···O6	6.9	H8···H1′(3′-G)	2.6
N7···N7	6.6	H8···H2′(5′-G)	3.7
O6···$N_1(NH_3)$(5′-G)	3.0	H8···H2″(5′-G)	4.6
O6···$N_2(NH_3)$(5′-G)	4.7	H8···H2′(3′-G)	3.9
O6···$N_1(NH_3)$(3′-G)	3.0	H8···H2″(3′-G)	4.3
O6···$N_2(NH_3)$(3′-G)	4.6		
Plane Angles (deg)			
$(PtN_4)_1/(PtN_4)_2$	21	$(PtN_4)_1$/5′-G	61
5′-G/3′-G	26	$(PtN_4)_2$/3′-G	65

Scheme 2. Schematic Representation of Observed Base/Base Orientations in Intrastrand Adducts[a]

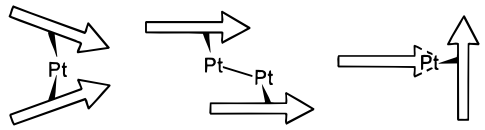

Head-to-Head Stepped-Head-to-Head Head-to-Side

[a] Head-to-head is "normal" arrangement for *cis*-DDP adducts, stepped head-to-head is observed for dinuclear platinum adducts, and the head-to-side arrangement is seen in hairpin adducts. See text for references.

Discussion

Structure of the (Pt,Pt)−Intrastrand Cross-Link. Because of the interesting biological properties of the 1,1/t,t bisplatinum complexes, and in particular their interaction with DNA, the structure of the (Pt,Pt)−d(GpG) intrastrand adduct of these compounds has been investigated in detail. The structures obtained by molecular modeling accord with the NMR results. Both NMR data and molecular modeling are consistent with a change around the glycosidic bond toward a *syn* orientation for G(2), whereas G(1) remains *anti*. This is a principal difference with respect to the *cis*-DDP adduct where the platinated GG moiety usually shows the well-described *anti*,*anti* conformation for both guanines in a head-to-head fashion with the 5′-G deoxyribose ring adopting a 100% N-type conformation.[11,12,23−26] Thus, the structure of the dinuclear platinum intrastrand GG cross-link differs markedly from its *cis*-DDP analog. A *syn* orientation of G(2) is generally not observed for the GG chelate of *cis*-DDP, although a few platinated hairpin-like structures do show an *anti/syn* arrangement resulting in a "head-to-side" conformation of the G bases (See Scheme 2).[45,54,55] Interestingly, the repeated 3′-syn → 5′-anti motif in $d(CGG)_n$ oligonucleotides has recently been shown to produce hairpin-like structures.[56] These results suggest the utility of dinuclear compounds in inducing and maintaining a hairpin-like structure in such sequences.

The sugar conformations of G(1) and G(2) are also different from the *cis*-DDP structure. The sugar conformation of G(1)

(54) Yohannes, P. G.; Zon, G.; Doetsch, P. W.; Marzilli, L. G. *J. Am. Chem. Soc.* **1993**, *115*, 5105−5110.
(55) Iwamoto, M.; Mukunda, S. J.; Marzilli, L. G. *J. Am. Chem. Soc.* **1994**, *116*, 6238−6244.
(56) Mitas, M.; Yu, A.; Dill, J.; Haworth, I. S. *Biochemistry* **1995**, *34*, 12803−12811.

is not 100% N-type in [1,1/t,t]GG ($n = 3$ and 6), although it is for [1,1/t,t, $n = 2$]. Compared to unplatinated DNA, which generally has 80−100% S, the population of S conformer of both G(1) and G(2) is significantly reduced upon binding of 1,1/t,t complexes.

Biological Implications. The steric demands of bifunctional binding of *cis*-DDP to two adjacent guanines contribute to the rigid directed bend in DNA induced by the intrastrand adduct.[11] This situation is reflected in the N-type conformation of the 5′-G and the *anti/anti* sugar arrangement. For *cis*-DDP analogs, deviation from these structural features may result in unusual conformations such as the hairpin-like structures observed by Marzilli.[45,54,55] The bending of a site-specific (Pt,Pt)−d(GpG) intrastrand adduct is characterized as a flexible bend.[22] In the present case, the inherent flexibility caused by monofunctional binding of both Pt atoms to their respective guanine bases is apparent in the structure. The stepped head-to-head configuration would not be expected to be sterically rigid. There is sufficient flexibility within the diamine chains that chain length, while it may affect some details of dinucleotide binding, does not alter greatly the bending in an oligonucleotide.

Bending induced by the *cis*-DDP intrastrand adduct is recognized by proteins containing the HMG-domain motif. A critical feature for such protein recognition is directed bending of DNA into the major groove.[10,57] The flexible bending caused by dinuclear platinum complexes allows us to identify a structural feature (flexibility) that would *prevent* such bending and thus allow for systematic "bypass" of protein recognition. The presence of such a bypass could be of great importance in contributing to the cytotoxicity of dinuclear platinum complexes in *cis*-DDP-resistant cells, where the mechanism of resistance involves enhanced repair of the *cis*-DDP intrastrand adduct.[58,59] A very interesting observation is the reduced binding affinity of the HMG-protein to the global DNA lesions of 1,1/t,t complexes.[18,21] The present results may help explain the structural basis for this observation. The biological role of HMG and its relevance with respect to cytotoxicity, resistance, and repair is, at present, not known. Interaction of HMG with platinated DNA could initiate the repair process or, alternatively, protect the platinated site from repair proteins.[10,60] The observation that 1,1/t,t lesions are not recognized by HMG but do show antitumor activity in cDDP-resistant cell lines suggests that, for these cells, HMG binding is not required for antitumor activity. Perhaps in cDDP-resistant cells, HMG binding induces the repair process instead of shielding the cross-links from repair. One might even speculate that in cDDP-resistant cells proteins other than HMG are present, which recognize other lesions, such as the ones induced by the 1,1/t,t compounds, and protect these adducts from repair.

The induction and maintenance of the *syn* conformation of a platinated guanine could also have consequences for the structures of (Pt,Pt) interstrand cross-links. The formation and irreversibility of Z-form poly[dG−dC] poly[dG−C] induced by dinuclear platinum complexes,[21,61−64] as well as the influence of monofunctional compounds such as [Pt(dien)] on the B → Z transition,[65−67] is most likely to involve a *syn* conformation of the guanine bases upon Pt binding, since an alternating *anti* (cytosine)−*syn* (guanine) repeating unit is required for induction of the left-handed form.[68] The unusual structures of 1,2-interstrand cross-links elucidated recently by ^{1}H NMR spectroscopy for both mononuclear *cis*-DDP[69] and one of the dinuclear compounds[70] may in part be a reflection of the *syn* sugar conformation. Thus, these studies demonstrate that it is possible to design a drug that alters DNA binding and may, thereby, alter antitumor activity and protein recognition or repair in comparison to cis-DDP.

Acknowledgment. This research is funded by American Cancer Society Grant DHP-2E and is sponsored by the Netherlands Organisation for Chemical Research (SON), and the Netherlands Foundation for Technical Research (STW), with financial aid of the Netherlands Organisation for the Advancement of Research (NWO).

Supporting Information Available: Figures of chemical shift of H8 versus pH for the GG-N7,N7 macrochelate structures (S1) and 1D ^{1}H NMR spectra of final products of the reaction of 1,1/t,t complexes with d(GpG) (S2) (2 pages). Ordering information is given on any current masthead page.

JA961823K

(57) Lilley, D. M. J. *Nature* **1992**, *357*, 282−283.
(58) Kašpárková, J.; Brabec, V. *Biochemistry* **1995**, *34*, 12379−12387.
(59) Kane, S. A.; Lippard, S. J. *Biochemistry* **1996**, *35*, 2180−2188.
(60) Lippard, S. J. *Proc. R. A. Welch Found.* **1993**, *37*, 49−62.
(61) Johnson, A.; Qu, Y.; van Houten, B.; Farrell, N. *Nucleic Acids Res.* **1992**, *20*, 1697−1703.
(62) Wu, P.; van Houten, B.; Qu, Y.; Farrell, N. *J. Inorg. Biochem.* **1994**, *54*, 207−220.
(63) Wu, P.; Kharatishvili, M.; Qu, Y.; Farrell, N. *J. Inorg. Biochem.* **1996**, *63*, 9−18.
(64) Kharatishvili, M.; Qu, F.; Farrell, N. *Biochemistry*, submitted.
(65) Ushay, H. M.; Santella, R. M.; Grunberger, D.; Lippard, S. J. *Nucleic Acids Res.* **1982**, *10*, 3573−3588.
(66) Malfoy, B.; Hartmann, B.; Leng, M. *Nucleic Acids Res.* **1981**, *9*, 5659−5669.
(67) Parkinson, G. N.; Arvanitis, G. M.; Lessinger, L.; Ginell, S. L.; Jones, R.; Gaffney, B.; Berman, H. M. *Biochemistry* **1995**, *34*, 15487−15495.
(68) Wang, A. H.-J.; Quigley, G. J.; Kolpak, F. J.; Crawford, J. L.; van Boom, J. H.; van der Marel, G.; Rich, A. *Nature* **1979**, *282*, 680−686.
(69) Huang, H.; Zhu, L.; Reid, B. R.; Drobny, G. P.; Hopkins, P. B. *Science* **1995**, *270*, 1842−1845.
(70) Yang, D.; van Boom, S. S. G. E.; Reedijk, J.; van Boom, J. H.; Farrell, N.; Wang, A. H.-J. *Nat. Struct. Biol.* **1995**, *2*, 577−586.